Relationship Between Pore Structure and ^{1}H-NMR Relaxation Times in TiO_2/Poly(dimethylsiloxane) and $CaCO_3$/Poly(dimethylsiloxane) Composite Powders

F. M. VICHI,[1] F. GALEMBECK,[1] T. K. HALSTEAD,[2] M. A. K. WILLIAMS[2]

[1] Instituto de Química, Universidade Estadual de Campinas, Caixa Postal 6154, 13081-970 Campinas, SP, Brazil

[2] Department of Chemistry, University of York, Heslington YO1 5DD, United Kingdom

Received 5 August 1998; accepted 10 May 1999

ABSTRACT: Titanium(IV) oxide/polydimethylsiloxane (PDMS) and calcium carbonate/PDMS composite powders were obtained by adsorption of the polymer from a chloroform solution onto the inorganic particles followed by a thermal treatment. The composites were characterized by ^{1}H-NMR relaxation and porosimetry. The composites present shorter spin–lattice (T_1) and spin–spin (T_2) proton relaxation times than silica-reinforced PDMS, and the activation energies for the motions that cause spin–lattice relaxation are 5.8, 4.9, and 0.72 kJ mol^{-1} for TiO_2/PDMS, $CaCO_3$/PDMS, and neat PDMS, respectively, revealing the greater rigidity of the polymer chains within the composite. Spin–spin relaxation (T_2) measurements of the composites showed a major component with a shorter T_2 and a minor component with a longer T_2. The intensity ratio of these two components is very close to the ratio between the amount of polymer that remains between the particles and that penetrating the particle pores as measured by Hg intrusion porosimetry. The shorter T_2 component was thus assigned to polymer interspersed among the particles, while the longer T_2 component was assigned to polymer within the particle pores. © 1999 John Wiley & Sons, Inc. J Appl Polym Sci 74: 2660–2666, 1999

Key words: polydimethylsiloxane/inorganic powder composites; proton NMR relaxation; porosity

INTRODUCTION

Polymer coated inorganic particles (PCIPs) are an important class of materials that have a good coupling between the organic and inorganic phases. Among the advantages presented by polymer encapsulated particles, two are especially important: good dispersibility in organic media and their suitability for compression-molding operations.[1] PCIPs has several applications, for example, the improvement of tensile strength in rubbers,[2] the manufacture of diaphragm materials for loudspeakers,[3] and pigmented paint film improvement.[4]

A simple procedure for obtaining PCIPs was described by Tanaka and coworkers.[5] It consists of suspending the particles in a polymer solution using an organic solvent. The encapsulation is achieved when the solvent is evaporated. In this case, however, one cannot be assured of the formation of chemical bonds between the particle and the polymer, the absence of which may lead to poor polymer–particle adhesion. TiO_2 particles coated with polymers were obtained by polymerization of monomers adsorbed on the oxide sur-

Correspondence to: F. Galembeck.
Contract grant sponsors: FAPESP; CAPES; British Council.

Journal of Applied Polymer Science, Vol. 74, 2660–2666 (1999)
 CCC 0021-8995/99/112660-07

face, yielding substrates for the paint industry. In this particular field the demand for water-soluble paints increased in the last decade because they pollute less than conventional paints based on organic solvents. One of the problems encountered in latex-based paints is the agglomeration of pigment and/or filler particles during film formation.[6] The encapsulation of a hydrophilic pigment by a polymer increases the compatibility with the organophilic adhesion agent, thus preventing agglomeration. This leads to a better film with higher brilliance and adhesion, which is also more stable, durable, and weather resistant.[7–10]

A way of assuring the formation of particle–polydimethylsiloxane (PDMS) bonds was described in recent work from this laboratory.[11,12] After the removal of the solvent, PDMS-coated inorganic particles are heated and chain scission produces reactive chain ends that bind to the particle surfaces. Chemical bonding is thus obtained between the two phases. In this case the presence of chemical bonds between the polymer and oxide is of great importance to guarantee a strong bonding between two incompatible phases.

The preparation of silanized inorganic surfaces is extensively described in the literature.[13–15] Existing procedures usually involve the use of organosilanes as coupling agents,[16–18] which undergo hydrolysis and form reactive silanol groups. These react with hydroxyl groups (e.g., from a glass surface) and form oxane bonds between the silane and the glass surface.

The use of a stable PDMS polymer instead of the reactive and somewhat volatile silanes is desirable when large-scale operations are necessary. Therefore, we concentrated on the use of PDMS instead of toxic silanes.

It has been shown that the bonding of PDMS to a hydroxylated inorganic surface can be brought about by thermal activation when the polymer is in contact with glass surfaces and iron(III) oxide particles.[6] The process is ascribed to siloxane chain breaking,[7,13] followed by newly formed chain-end reactions with surface reactive groups such as Fe—OH. Above 250°C and in the presence of air, PDMS undergoes two main transformations[19]: chain heterolytic cleavage, yielding reactive Si— and O— groups, which may in turn react with hydroxylated surfaces and other segments of the polymer chain. In the latter case the resulting products are crosslinked networks and low molecular weight oligomers (both cyclic and linear); another possibility is the oxidation of the methyl end groups, which in turn react with other chain segments leading to crosslinking through methylene or siloxane bridging. The complexity of the chemistry involved in these processes makes it difficult for these systems to be characterized by most techniques that are normally applied in polymer science. The use of NMR spectroscopy, however, provides an insight into both the chemical composition and the structure of Si compounds in a solid. The theories for the NMR relaxation behavior of polymers are extensive and give a special importance to some parameters, especially the degree of crosslinking and entanglements.[20–23]

In this article we study the relaxation behavior and pore structure of TiO_2/PDMS and $CaCO_3$/PDMS composite powders and relate them by use of a simple model.

EXPERIMENTAL

PDMS (1000 cSt fluid, Dow Corning) was added to chloroform (Merck) to form a 50% (v/v) solution, which was stirred by tumbling for 2 h. Powdered titanium(IV) oxide (Riedel-de-Häen) was added to this solution to obtain an oxide/PDMS ratio of 1 : 1 (w/w). The resulting slurry was mixed by tumbling for 18 h at room temperature (25°C). The chloroform was then removed by evaporation and the oxide/PDMS mixture was placed in a preheated oven at 265°C for 1 h, then removed from the oven and allowed to cool to room temperature. The composite powder was then placed in a cellulose cup and extracted with chloroform in a Soxhlet extractor for 18 h to remove excess PDMS. After the extraction the powder was dried in an oven at 120°C for 6 h.

The resulting TiO_2/PDMS composite was a white, free-flowing, highly hydrophobic powder that can be easily dispersed in apolar solvents, but not in polar solvents.

Chemical analysis was performed on a Perkin–Elmer PE-2400 CHN analyzer. The PDMS content was determined from the carbon content, assuming that all carbon comes from the polymer. Density measurements were made in a Micromeritics 1305 helium multipicnometer, and pore size distribution data were obtained in a Micromeritics 9320 mercury intrusion pore sizer. Transmission electron micrographs were obtained on a Zeiss CEM-902 instrument. Proton NMR spectroscopy was performed on a Bruker MSL-300 spectrometer operating at 300.13 MHz. The sam-

Table I PDMS Content, Density, and Surface Area for TiO_2, TiO_2/PDMS, $CaCO_3$, and $CaCO_3$/PDMS

	PDMS Content (%)[a]	Density (g cm^{-3})	Surface Area (m^2 g^{-1})
TiO_2	0.0	4.91 ± 0.02	8.88 ± 0.04
TiO_2/PDMS	11.2	3.17 ± 0.04	3.45 ± 0.07
$CaCO_3$	0	3.04 ± 0.03	10.73 ± 0.11
$CaCO_3$/PDMS	6.0	3.04 + 0.02	2.76 ± 0.09

[a] Calculated from the carbon content obtained by chemical analysis.

ples were placed in glass NMR tubes with a 5-mm external diameter. Spin–lattice relaxation times (T_1) were obtained by the inversion recovery technique. Spin–spin relaxation times (T_2) were measured using the CPMG sequence. The pulse lengths were 13.3 (90°) and 26.6 μs (180°). Solid-state (cross polarization) magic angle spinning NMR (CP MAS-NMR) spectra were obtained for ^{29}Si and ^{13}C in a Bruker CXP 300 spectrometer operating at 59.63 and 75.48 MHz, respectively. The samples were spun at 4.5 kHz in Bruker aluminum oxide rotors. Contact times of 8 (^{29}Si) and 1 ms (^{13}C) were used for maximum magnetization transfer with 1- and 2-s pulse intervals, respectively. The acquisition times were 10 (^{29}Si) and 29 ms (^{13}C). The spectra were obtained after 2.2×10^4 accumulations. Tetramethylsilane (TMS) was used for $\delta = 0$ ppm adjustment for both nuclei.

RESULTS AND DISCUSSION

Physicochemical Characterization

The physicochemical properties of the TiO_2/PDMS composite particles are summarized in Table I.

It can be seen that the incorporation of PDMS decreases the particle density (PDMS is far less dense than TiO_2), as well the powder surface area, because of the penetration of PDMS into the pores of the powder. The PDMS content also reveals that, although a 50% (w/w) polymer/powder ratio is used in the preparation, only 11.2% of the polymer remains in the composite. This can be ascribed to two factors: there is a saturation of the surface with polymer chains, and a part of the adsorbed polymer is eliminated as low molecular weight oligomers during the heating process.

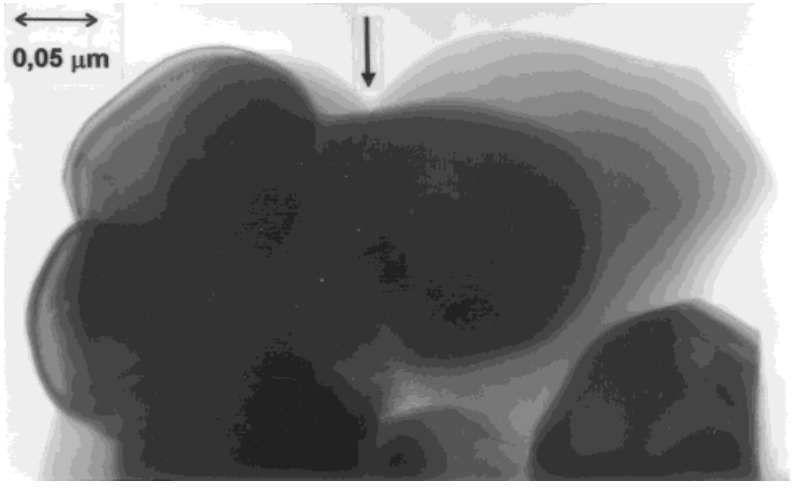

Figure 1 Transmission electron micrograph of TiO_2/PDMS particles. The polymer layer at the edge of the particles is indicated by the arrow.

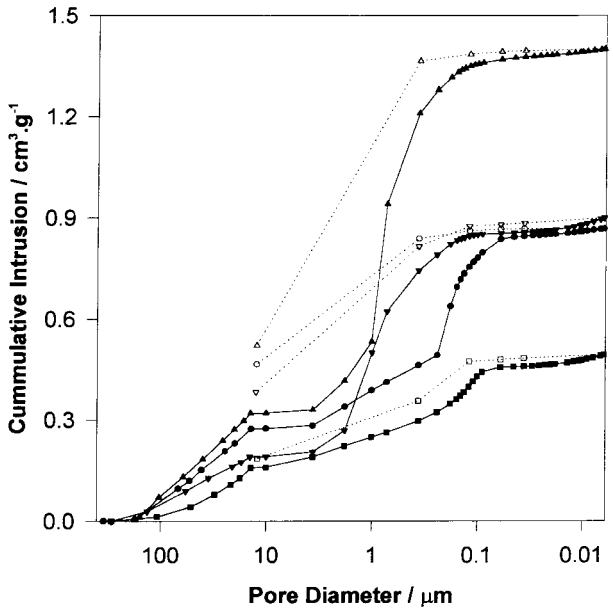

Figure 2 Cumulative intrusion versus pore diameter for TiO_2 (●) intrusion and (○) extrusion; TiO_2/PDMS (■) intrusion and (□) extrusion; $CaCO_3$ (▲) intrusion and (△) extrusion; and $CaCO_3$/PDMS (▼) intrusion and (▽) extrusion.

Transmission Electron Microscopy (TEM)

The encapsulation of the oxide particles by the polymer can be observed by TEM. Figure 1 shows a representative TEM micrograph of TiO_2/PDMS composite particles in which a contrast region can be seen at the particle edges. This is assigned to a PDMS layer having an approximate thickness of 5–6 nm. The particles are aggregated and kept together by the polymer interspersed among them. The $CaCO_3$/PDMS composite shows similar behavior.

Pore Structure

The pore structure of the powders can be assessed from the data in Figure 2 that presents the curve of differential intrusion versus pore diameter. The integration of these curves gives the total intrusion volume for each sample. However, because the mean particle size is known from the TEM, this intrusion volume can be divided into two regions: interparticle intrusion (mercury interspersed in the spaces among the particles) and intraparticle intrusion (mercury that penetrates within the particle pores). This is achieved by setting the integration limits according to the particle size as determined by TEM. The integration limits are therefore 350 and 0.1 μm for the interparticle intrusion and 100 and 6 nm for the interparticle intrusion. The results are presented in Table II.

The values in Table II show that there is a significant reduction in the intrusion volume when PDMS is incorporated in the TiO_2 particles. We observed that, although most of the incorporated polymer is located between the particles, there is also a reduction in the intraparticle intrusion volume, meaning that some polymer also penetrates into the pores.

NMR Spectroscopy

MAS-NMR

The ^{13}C-CP MAS-NMR spectrum of the TiO_2/PDMS composite is presented in Figure 3. The carbonate composite presents a very similar spectrum. Only one peak is observed at δ = 1.2 ppm, corresponding to the methyl groups of the PDMS chain. No other peak is observed, indicating the absence of C—O—Ti and C—O—Si groups, which would present peaks at about 18 ppm.[24] The absence of peaks at $\delta = \sim 66$ and 12–14 ppm, corresponding to O—CH_2— and Si—CH_2— groups, respectively, reveals that methylene bridging does not occur.

The ^{29}Si spectrum of the TiO_2/PDMS composite is shown in Figure 4. Again, the carbonate com-

Table II Interparticle and Intraparticle Intrusion Volumes

	Intrusion Volume (mL g^{-1})		
Sample	Interparticle Space	Intraparticle Space	Total
TiO_2	0.825 (91.0)	0.081 (9.0)	0.906 (100)
TiO_2/PDMS	0.448 (90.8)	0.045 (9.2)	0.493 (100)
$CaCO_3$	1.289 (87.3)	0.187 (12.7)	1.477 (100)
$CaCO_3$/PDMS	0.848 (84.8)	0.152 (15.2)	1.000 (100)

The values in parentheses are the percentile figures.

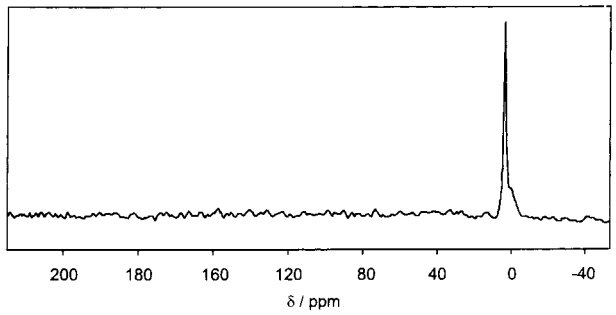

Figure 3 ^{13}C-MAS-NMR spectrum of the TiO_2/PDMS composite.

posite presents a very similar spectrum, although less intense. A number of peaks are observed in contrast with a spectrum of neat PDMS, which shows only one peak at $\delta = 21.6$ ppm.[25] The diversity in Si functionality observed in Figure 4 reflects the transformations that occur in the polymer during the heat treatment. The peaks observed at $\delta = -10$ and -11 ppm can be ascribed to low molecular weight cyclic oligomers formed during the thermal treatment.[18,26] It is possible that a fraction of these oligomers remains in the composite, which are either trapped in pores or bound to the inorganic surface. The presence of peaks at $\delta = -58$ and -66 ppm, corresponding to trisubstituted Si atoms, and at $\delta = -109$ ppm, corresponding to tetrasubstituted Si atoms, confirms the formation of crosslinks. Another interesting feature in the spectrum in Figure 4 is the presence of a weak peak at $\delta = -24.3$ ppm. Although very weak, this peak appears in several spectra obtained for this sample. Following Diré and coworkers,[27,28] we attribute this peak to the presence of Si—O—Ti bonding, confirming the formation of chemical bonds between the polymer and the inorganic phase.

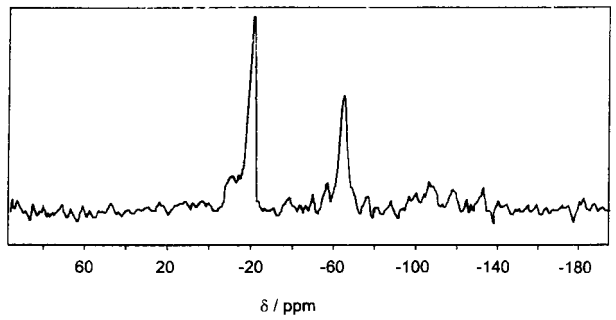

Figure 4 ^{29}Si-MAS-NMR spectrum of the TiO_2/PDMS composite.

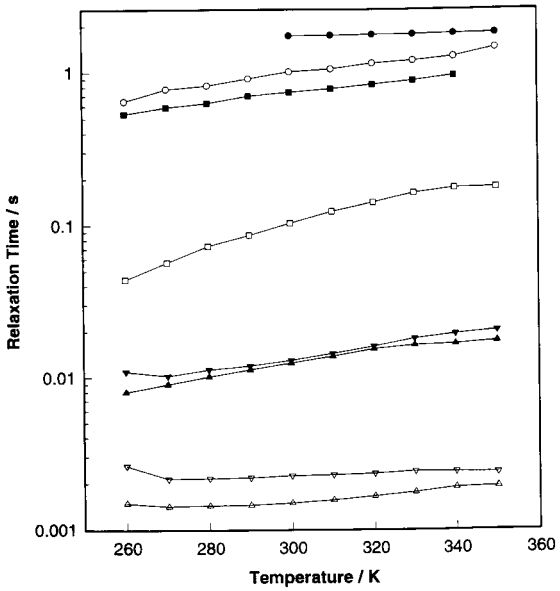

Figure 5 Relaxation times observed for PDMS, TiO_2/PDMS, and $CaCO_3$/PDMS. (●) PDMS T_1, (○) TiO_2/PDMS T_1, (■) $CaCO_3$/PDMS T_1, (□) PDMS T_2, (▲) TiO_2/PDMS T_2 long component, (△) TiO_2/PDMS T_2 short component, (▼) $CaCO_3$/PDMS T_2 long component, and (▽) $CaCO_3$/PDMS T_2 short component.

^{1}H-NMR: Spin–Lattice (T_1) and Spin–Spin (T_2) Relaxation

Spin–lattice relaxation times (T_1) were obtained through the inversion recovery pulse sequence and spin–spin relaxation times (T_2) were obtained using the CPMG pulse sequence. The results are presented in Figure 5.

In their work about elastomers reinforced with *in situ* precipitated silica, Garrido et al.[29] observed T_1 values of 1.19–1.26 s for PDMS samples containing 1.9–4.7 wt % silica. Their figures were obtained at room temperature and can be compared to our values obtained at 300 K, which are 1.01 ± 0.01 s for TiO_2/PDMS, 0.74 ± 0.02 s for $CaCO_3$/PDMS, and 1.73 ± 0.08 s for the neat polymer. The shorter values observed for our composites reflect two basic differences between our materials and the silica-reinforced elastomers. First, in our work the amount of inorganic material is much larger than in these elastomers, so that the fraction of polymer chains in direct contact with the inorganic surface is larger. This leads to a more rigid structure and therefore to shorter T_1 values. Second, the PDMS layers obtained by thermal treatment are crosslinked, which also contribute to the increase in rigidity. Furthermore, the shorter value observed for the

carbonate composite seems to indicate a higher degree of polymer crosslinking, possibly induced by the more basic carbonate.

The T_1 is sensitive to molecular motions that occur at frequencies close to the resonance frequency. In the present case these probably consist of reorientation about the C_3 axis of the methyl groups, because of the rotation of short main chain segments.[30,31] At room temperature the rotation of the methyl groups about the Si—C bond is too rapid to contribute effectively to spin–lattice relaxation.

The energy of activation for the motions responsible for spin–lattice relaxation can be determined from the slope of ln T_1 versus the reciprocal temperature plots.

When the motions are described by a single correlation time (i.e., the correlation function is a single exponential), the slopes correspond to $-E_a/R$. The values obtained were 5.8 ± 0.2, 4.9 ± 0.2, and 0.72 ± 0.03 kJ mol^{-1} for TiO_2/PDMS, $CaCO_3$/PDMS, and neat PDMS, respectively. The larger values observed for the composites reflect the immobilization of the polymer over the inorganic surfaces, as well as the presence of crosslinks. The resulting chains are more rigid, and the motions that cause relaxation (rotation of chain segments about Si—O bonds) are more hindered than in the neat polymer. We also note that the activation energies for the composites are higher than kT, which ranges from 1.7 to 2.9 kJ mol^{-1} in the temperature interval of this study. Inversely, neat PDMS presents an activation energy lower than kT. This means that the motions responsible for spin–lattice relaxation are unrestricted in the neat polymer within the temperature interval of this study, but they are hindered in the particle-bound PDMS.

Spin–spin relaxation times were obtained for temperatures ranging from 230 to 350 K. To determine the equation that would best fit the data, a number of exponential equations were applied. For both composites a double exponential behavior was observed, and the data can be fitted to the equation

$$I = (1 - f)[(\exp - t/T_{2a})] + f[(\exp - t/T_{2b})] \quad (1)$$

where T_{2a} and T_{2b} are two distinct relaxation times and f is the polymer fraction with the shorter relaxation time. The results can be seen in Table III.

Garrido et al.[29] also observed two values of T_2 for their reinforced elastomers. The room temperature values ranged from 0.79 to 0.86 ms for the shorter component and 69 to 221 ms for the shorter and longer components, respectively. Again our values are lower: TiO_2/PDMS presents 0.12 ± 0.03 and 15 ± 2 ms for the shorter and longer components, respectively, and for $CaCO_3$/PDMS the observed values are 0.13 ± 0.03 and 22 ± 1 ms, respectively.

Table III Fractions f of Polymer with Shortest and Longest T_2 in Composites

Sample	f_{shortest} (%)	f_{longest} (%)
TiO_2/PDMS	91.4	8.6
$CaCO_3$/PDMS	83.0	17.0

Garrido et al. interpreted their results in terms of a major component with the shorter T_2 corresponding to the chain segments forming the PDMS network and a minor component and a longer T_2 corresponding to ethyl groups from partly hydrolyzed TEOS.[29] Because in the present case the PDMS was not prepared by hydrolysis, other explanations must be sought. We envision two possibilities.

Spin–Spin Relaxation and Pore Structure. In Table II we observe that in the TiO_2/PDMS composite 90.8% of the polymer is located between individual particles, while 9.2% effectively penetrates the particle pores. If we calculate the value for the fraction of PDMS with shorter T_2 at 300 K from eq. (1) we see that this corresponds to 91.4%, and the fraction with longer T_2 corresponds to 8.6% of the polymer. For the $CaCO_3$/PDMS composite, 84.8% of the polymer is located between the particles and the remaining 15.2% is located within the particle pores. From eq. (1) the fraction of polymer with shorter T_2 corresponds to 83.0%, and the fraction with longer T_2 corresponds to 17.0%. The resemblance between each of the two pairs of values is striking, suggesting that the shorter T_2 segments are located in between the particles while the longer T_2 segments are located within the pores. Polymer crosslinking and surface immobilization, which cause an increase in chain rigidity and therefore lead to shorter T_2, occur through the cleavage of Si—O bonds of the main chain, followed by a recombination of the newly formed reactive chain ends. In the presence of air the elimination of volatiles is accelerated and crosslinking occurs because of the elimination of methyl groups through oxidation.[26]

The polymer contained within the pores is less exposed to air, being less subject to the formation of T or Q siloxane groups than the fraction that remains between the particles, and thus has a longer T_2. However, some degree of crosslinking does occur, as well as bonding to the inorganic surface, as can be seen from the value of T_2 (15 ms), which is shorter than that observed for the neat polymer by 1 order of magnitude.

Presence of Low Molecular Weight Species. The decomposition of PDMS during the heat treatment leads to the formation of low molecular weight cyclic and linear oligomers.[26] These oligomers are not subject to the motion restrictions observed in the high molecular weight polymers and therefore have longer relaxation times. If some of these oligomers become trapped within the pores during the heat treatment, they could be responsible for the longer T_2 component.

It should be noted, however, that possibilities A and B are not mutually exclusive and the observed behavior may be the result of a combination of them.

CONCLUSION

PDMS is strongly immobilized in TiO_2/PDMS and $CaCO_3$/PDMS composite particles. This is due to the formation of tri- and tetraoxygenated (T and Q) Si atoms, which is consistent with polymer crosslinking, as well as polymer–particle bonding. Spin–spin relaxation does not follow a single exponential pattern. Out of the models examined for the interpretation of the relaxation results, a good fit was obtained with a two-sites model in which the slow-relaxing (and minor component) polymer is within the particle pores, while the faster relaxation is due to polymer immobilized in between the particles.

F.G. acknowledges CNPq, FAPESP, and PRONEX/FINEP/MCT for continuing support.

REFERENCES

1. Mosbach, K.; Andersson, L. Angew Makromol Chem 1977, 57, 225.
2. Nakatsuka, T.; Kawasaki, H.; Yamashita, K. J Colloid Interface Sci 1981, 82, 298.
3. Ono, T. Org Coatings 1986, 18, 279.
4. Eden, J.; Trksak, R.; Williams, R. U.S. Pat. 4,755,397 A, 1988.
5. Tanaka, M.; Hosogai, K.; Yamada, T. Shikizai Kyokaishi 1988, 61, 543.
6. Ono, T. Org Coatings 1986, 18, 279.
7. Solc, J. Eur. Pat. Applic. 0 054 832 A2, 1981.
8. Maslosh, V. Z.; Popov, A. F.; Pashchenko, V. L.; Kudyukov, Y. P.; Moroz, V. A.; Bukhan'ko, A. I. Russ. Pat. 1652324 A1, 1991.
9. Templeton-Knight, R. L. J Oil Colour Chem Assoc 1990, 73, 459.
10. Templeton-Knight, R. L. Chem Ind 1990, 16, 512.
11. Botter, W., Jr.; Soares, R. F.; Galembeck, F. J Adhesion Sci Technol 1992, 6, 781.
12. Soares, R. F.; Leite, C. A. P.; Botter, W., Jr.; Galembeck, F. J Appl Polym Sci 1996, 60, 2001.
13. Ballistreri, A.; Garozzo, D.; Montaudo, G. Macromolecules 1984, 17, 1312.
14. Allen, K. W. J Adhesion Sci Technol 1992, 6, 23.
15. Zhang, S.; Schindler, B.; Nicholson, G.; Bayer, E. J High Resolut Chromatogr 1995, 18, 579.
16. Grundemeier, G.; Matheisen, E.; Stratmann, M. J Adhesion Sci Technol 1996, 10, 573.
17. Plueddemann, E. P. Silane Coupling Agents; Plenum Press: New York, 1982.
18. Thomas, T. H.; Kendrick, T. C. J Polym Sci 1969, 7, 537.
19. Plueddemann, E. P. Encyclopedia of Polymer Science and Engineering; Wiley-Interscience: New York, 1985; Vol. 4, p 204–308.
20. Abragam, A. The Principles of Nuclear Magnetism; Clarendon Press: Oxford, U.K., 1961.
21. Cohen-Addad, J. P.; Doruard, M.; Herz, H. J Chem Phys 1982, 76, 2744.
22. Cohen-Addad, J. P. J Chem Phys 1974, 60, 2440.
23. Kimmich, R. Colloid Polym Sci 1982, 260, 911.
24. Loy, D. A.; Mason, G. M.; Maugher, B. M.; Myers, S. A.; Assinik, R. A.; Shea, K. J. Chem Mater 1996, 8, 656.
25. Soares, R. F. M.Sc. Thesis, University of Campinas, Campinas, Spain, 1997.
26. Kendrick, T. C.; Parbhoo, B.; White, J. W. In The Chemistry of Organosilicon Compounds; Patai, S.; Rappoport, Z., Eds.; Wiley: Chichester, U.K., 1989; Vol. 2, p 1335.
27. Diré, S.; Babonneau, F.; Carturan, G.; Livage, J. J Non-Cryst Solids 1992, 147–148, 62.
28. Babonneau, F.; Maquet, J.; Diré, S. Polym Prepr 1993, 34, 246.
29. Garrido, L.; Mark, J. E.; Sun, C. C.; Ackerman, J. L.; Chang, C. Macromolecules 1991, 24, 4067.
30. Powles, J. G.; Hartland, A.; Kail, J. A. E. J Polym Sci 1961, 55, 361.
31. Cuniberti, C. J Polym Sci Polym Phys Ed 1970, 8, 2051.